The Journal of Antibiotics (2018) 71:731–740
https://doi.org/10.1038/s41429-018-0061-z

JARA Japan Antibiotics Research Association
The Society for Actinomycetes Japan

ARTICLE

The activities of wortmannilactones against helminth electron transport chain enzymes, structure-activity relationships, and the effect on *Trichinella spiralis* infected mice

Wen-Cai Liu[1] · Yi-Xin Ren[2] · Ai-Yu Hao[3] · Sun Yu[1] · Xuan Shi[1] · Xue-Qiang Zhang[2] · Yan Xing[1] · Zhi-Long Xiu[1] · Yu Cui[2] · Yue-Sheng Dong[1]

Received: 27 November 2017 / Revised: 13 March 2018 / Accepted: 2 April 2018 / Published online: 24 April 2018

Abstract

Biotransformation of wortmannilactone F (**3**) using the marine-derived fungus DL1103 generated wortmannilactone M (**1**), a novel analog of wortmannilactone, which was a reduction product of **3** at the C-3 carbonyl group. The in vitro inhibitory activities of 10 wortmannilactones, including **1**, against electron transport enzymes indicated that all the wortmannilactones were selective inhibitors of NADH-fumarate reductase and NADH–rhodoquinone reductase. The structure–activity relationship analysis showed that the relative configuration of C1" and C5", the positions of double bonds, the oxygen atoms in the dihydropyran moiety, and the keto-carbonyl group in the oxabicyclo-[2.2.1]-heptane moiety were important to the inhibitory activity of wortmannilactones. In vivo studies indicated that **3** significantly decreased the number and size of adult worms in *Trichinella spiralis*-infected mice in a dose-dependent manner. Notable changes in the cuticle and microvilli of *T. spiralis* were also observed. Our data provided useful information in the research and development of polyketides with dihydropyran and oxabicyclo [2.2.1] heptane moieties as antihelminthics.

Introduction

Parasitic helminth worms remain a severe threat to human health in developing nations and also limit production of livestock animals worldwide [1, 2]. Infections by these worms lead to a global burden of diseases, including schistosomiasis and filariasis, and cause serious economic loss to animal husbandry [1, 3]. Although several strategies are currently available to control helminth infection, antihelminthics still provide the mainstay approach for worm control. Several classes of antihelminthics have been applied in veterinary and human medicine for the control of nematodiasis, including nicotinic agonists (levamisole) [4], macrocyclic lactones (avermectin) [5, 6], benzimidazoles (albendazole) [7], and praziquantel [8]. However, due to the emergence of resistance to the currently used anti-helminthics, new pharmaceutical products that are parasite specific and minimally toxic to the host are urgently needed [9, 10].

Mitochondria are essential organelles involved in the oxidative phosphorylation for energy metabolism. In order to adapt to the low-oxygen conditions in the host body, parasites have evolved a distinct energy metabolic system from that of host mammals. Research on electron transport enzymes of parasitic helminths has shown that the mitochondrial NADH-fumarate reductase system (NFRD), which is composed of NADH–rhodoquinone reductase (complex I) and rhodoquinol–fumarate reductase (complex II), plays an important role in the anaerobic energy metabolism of adult helminths [11, 12]. The differences in the energy metabolism between the host and helminth make the NFRD an attractive therapeutic target of helminthiasis [13, 14]. The screening of inhibitors against helminth

Electronic supplementary material The online version of this article (https://doi.org/10.1038/s41429-018-0061-z) contains supplementary material, which is available to authorized users.

✉ Yu Cui
dlcuiyu@dlmedu.edu.cn

✉ Yue-Sheng Dong
yshdong@dlut.edu.cn

[1] School of Life Science and Biotechnology, Dalian University of Technology, Dalian, Liaoning 116024, China

[2] Department of Parasitology, College of Basic Medical Sciences, Dalian Medical University, Dalian, Liaoning 116044, China

[3] Dalian Institute for Drug Control, Dalian, Liaoning 116021, China

mitochondrial electron transport enzymes has also gained more attention [15].

Prugosenes, a new class of polyketides with a dihydropyran moiety, a conjugated pentaene, and an oxabicyclo [2.2.1] heptane moiety, were previously isolated from a solid rice medium fermentation of the marine fungus *Penicillium rugulosum*[16]. Ukulactone A, B, and C (**11**–**13**), the ethylated derivatives of prugosenes, from *Penicillium* sp. FKI-3389 and *Talaromyces* sp. FKI-6317, were found to exhibit selective inhibitory activities against NFRD and complex I [12, 17]. The different activities between ukulactones suggested that the configuration of the C-17 in the dihydropyran moiety and the keto-carbonyl group in the oxabicyclo [2.2.1] heptane moiety played an important role in the anthelmintic effects of the compounds. However, due to the limited number of ukulactones, the structure–activity relationship (SAR) of the compounds has not been explored in detail. The in vivo anthelmintic effects of these polyketides have not been thoroughly investigated either. Wortmannilactones E, F (**2**, **3**), the conjugated tetraene polyenes, were isolated from the culture of *Talaromyces wortmannii* by our group [18]. Recently, seven new wortmannilactones, wortmannilactones I-L (**4**–**7**) and wortmannilactones I1-I3 (**8**–**10**), with selective NFRD inhibitory activities were obtained by our group by adding epigenetic regulatory agents and changing culture media [19, 20]. These compounds showed good structural diversity, especially, in the dihydropyran moieties, which are beneficial for SAR analysis. However, the inhibitory activities of these wortmannilactones against complex I and complex II are still unknown.

In this paper, a new keto-carbonyl reduced product of wortmannilactones was prepared by a biotransformation approach. The SAR between wortmannilactones and electron transport enzymes were analyzed based on their inhibitory activities. Furthermore, in vivo studies were performed to evaluate the effect of **3** on *Trichinella spiralis* in a mouse model.

Results and discussion

Biotransformation of 3 and structure elucidation

In the biotransformation studies, a fungal strain named DL1103 was found to biotransform **3** to yield a new wortmannilactone derivative. A total of 2.0 g ethyl acetate extract was obtained from 2.0 L cultures using **3** as the substrate. After the isolation and purification, 6.4 mg white solid was obtained and named as wortmannilactone M (**1**). The DL1103 strain was identified as an *Aspergillus* sp, F1 by internal transcribed spacer (ITS) sequence comparison (supplemental material part 1).

Table 1 NMR data of wortmannilactone M in $CDCl_3$

Position	δ_H (Int., mult., *J* in Hz)	δ_C	HMBC (H→C)	NOESY
1		176.7		
2		60.6		
3	4.24 (1H, d, 8.8)	74.8	C-1	H-4, 2-CH_3, 6-CH_3
4	2.64 (1H, 8.8, 7.5, 1.7)	36.6	C-3	H-3, H-5, 4-CH_3
5	4.33 (1H, brs)	88.0	C-1, C-3	H-4, 6-CH_3
6		55.3		
1’	5.68 (1H, d, 14.5)	132.3	C-5, C-3”, 6-CH_3	H-3’
2’	6.28 (1H, dd, 14.0, 10.5)	133.6		
3’	6.18 (1H, dd, 13.6,10.5)	132.8		H-1’
4’	6.23 (1H, m)	132.9		H-6’
5’	6.26 (1H, m)	133.6		H-7’
6’	6.46 (1H, dd, 13.8, 11.0)	129.2		8’-CH_3, H-4’
7’	6.06 (1H, d, 11.0)	130.1	8’-CH_3, C-1”	H-5’
8’		135.7		
1”	4.31 (1H, s)	79.6	C-7’,C-8’, 8’-CH_3	8’-CH_3, 2”-CH_3, 5”-CH_3
2”		134.9		
3”	5.59 (1H, s)	129.4	C-1”, 2”-CH_3	2”-CH_3, 4”-CH_3
4”		69.0		
5”	3.77 (1H, q, 6.5)	75.1	C-1”, C-3”	
2-CH_3	1.16 (3H, s)	8.5	C-1, C-3, C-6	H-3
4-CH_3	1.09 (3H, d, 7.5)	9.1	C-3, C-5	H-4
6-CH_3	1.11 (3H, s)	15.5	C-2, C-5, C-1’	H-3, H-5
8’-CH_3	1.79 (3H, s)	14.0	C-1”,7’, 8’	H-1”, H-6’
2”-CH_3	1.54 (3H, s)	19.4	C-1”, 3”	H-1”, H-3”
4”-CH_3	1.16 (3H, s)	22.7	C-3”, C-5”	H-3”
5”-CH_3	1.17 (3H, d, 6.5)	14.7	C-4”	H-1”

NMR spectra were recorded at 500 MHz for ^1H and 125 MHz for ^{13}C

The molecular formula of **1** was determined to be $C_{26}H_{36}O_5$, based on positive high-resolution electrospray ionization mass spectrometry (HRESIMS) *m/z* ([M+H–H_2O]$^+$) *m/z* = 411.2528 (calculated: *m/z* = 411.2535) and *m/z* ([M+Na] $^+$) *m/z* = 451.2449 (calculated: *m/z* = 451.2460); the positive HRESIMS spectrum of **1** and its major fragments are summarized in Fig. S1.

Compound **1** has 9 degrees of unsaturation. The ^1H, ^{13}C nuclear magnetic resonance (NMR; Table 1) and heteronuclear single quantum correlation data suggested that **1** had the same number of carbon atoms as **3**, with one carbonyl group less, and signals for a new hydroxyl-methine

group at δ_C 74.8. Heteronuclear multiple-bond correlation (HMBC) data suggested that **3** had dihydropyran and tetraene moieties. The correlations from H-5 to C-1 and C-3, hydrogens of 2-CH_3 to C-1 and C-3, hydrogens of 4-CH_3 to C-3 and C-5, and hydrogens of 6-CH_3 to C-2, C-5, and C-1' were observed in HMBC data (Table 1, and Fig. S7). These data demonstrated the connections including C-2 to C-3, C-3 to C-4, C-4 to C-5, C-5 to oxygen atom of lactone, and C-6 to C-2 and C-5. Thus, **1** also had an oxabicyclo [2.2.1] heptane moiety. However, the correlations from δ_H 4.24 to C-1, H-5 to δ_C 74.8, and 4-CH_3 to δ_C 74.8 in HMBC spectra suggested that the carbonyl group of C-3 in the oxabicyclo [2.2.1] heptane moiety of **3** was reduced to a hydroxyl group in **1**. This result was supported by splitting of the ^{1}H NMR signal of H-4. This signal showed ddq splitting with coupling constants of 8.8 Hz, 7.2,and 1.7 Hz in **1** and dq splitting with coupling constants of 7.0 Hz and 2.0 Hz in **3** [18], suggesting that this hydrogen was further coupled with the single hydroxyl-methine hydrogen at H-3 with the coupling constant of 8.8 Hz. Thus, **1** was determined as the keto-carbonyl reduced product of **3** at C-3 (Fig. 1). These data also inferred that DL1103 produced a carbonyl reductase that could reduce the carbonyl group in the oxabicyclo [2.2.1] heptane moiety.

The relative configuration of **1** was identified by comparison of nuclear Overhauser effect spectroscopy (NOESY) and coupling constants with those of ukulactone C, which was also a carbonyl reduction product at C-3 in the oxabicyclo [2.2.1] heptane moiety. In compound **1**, the correlations from H-3 to H-4, and 6-CH_3 were observed in NOESY (Table 1, and Fig. S7), and the coupling constant between H-3 and H-4 was 8.8 Hz in ^{1}H NMR spectroscopy. In ukulactone C, on the contrary, only the correlation from H-3 to 4-CH_3 was observed, and the coupling constant of between H-3 and H-4 was smaller (3.5 Hz). These data showed that the relative configuration of C-3 was *R**, which was different from that of ukulactone C. The correlation from H-4 to H-5, and the correlation from H-3 to hydrogens of 2-CH_3, suggested the *2S**, *4R**, and *5R** configuration of the oxabicyclo [2.2.1] heptane moiety, which were the same as those in **3**. Similarly, the relative configurations of other carbons were also determined, and all the configurations were identical with those in **3** (Table 1 and Fig. S7). Thus, the relative configuration of **1** was 2*S**, 3*R**, 4*R**, 5*S**, *, 61"*S**, 4"*R**, and 5"*S**. The absolute configuration of **1** was identified by comparison between calculated and experimental electronic circular dichroism (ECD) spectra. The ECD spectrum of **1** was calculated using the time-dependent density functional theory (TDDFT) method (supplemental material part 4). The calculated CD spectrum of **1** agreed well with the experimental CD curve (Fig. 2), and thus the absolute configuration of **1** was 2*S*, 3*R*, 4*R*, 5*S*, 6*S*, 1"*S*, 4"*R*, and 5"*S*.

In vitro inhibition of electron transport enzymes by wortmannilactones

The half-maximal inhibitory concentration (IC_{50}) values of pyrvinium pamoate (PP) against NFRD, complex I, and complex II were 0.5 μM, 0.4 μM and 9 μM, respectively, which were consistent with the previous research [21], suggesting that the assay system is reliable. The IC_{50} value of **1** against NFRD was 13.5 μM, while the IC_{50} value of **1** against mammalian NADH oxidase was greater than 100 μM, showing selective inhibition. The inhibitory activities of the 10 wortmannilactones (**1–10**) against complex I and complex II from the submitochondrial particles of *Ascaris suum* are summarized in Table 2. All wortmannilactones exhibited inhibitory activities against complex I, with IC_{50} values ranging from 1.0 μM to 31.0 μM, but the inhibitory activities against complex II were all greater than 100 μM. The date indicated that all wortmannilactones could selectively inhibit the complex I of *A. suum*. In these compounds, **3** displayed the strongest inhibitory activity against complex I.

Structure−activity relationship between wortmannilactones and the activity of the compounds against electron transport enzymes

So far, the activities of ukulactone B and ukulactone C against complex I have not been reported. For wortmannilactones, the inhibitory activities against NFRD and complex I were both investigated and the trends of the activities were the same. Thus, we selected NFRD as the target enzyme to study the SAR within wortmannilactones and between wortmannilactones and ukulactones. Due to the different lengths of the polyene chain in wortmannilactones and ukulactones, which led to the mismatching of carbons and hydrogen numbers in comparison of SAR, a different numbering system from the previous publications was used in this paper (Fig. 1).

The wortmannilactones obtained showed more diversity in the dihydropyran moieties, which was beneficial for the study of the SAR. The planar structure of the dihydropyran moieties in **3**, **11**, and **12** were identical, and the difference was the configuration of C1" and C5". Both the configurations of C-1" of **3** and **11** were *S**, whereas the configuration of C-1" of **12** was *R**. Previous study suggested that the configuration of C-1" in ukulactones might play an important role in the activity against NFRD based on the fact that the alteration from 1"*S** (**11**) to 1"*R** (**12**) resulted in an inhibitory activity decreased by around 200-fold. However, in this study, the NFRD inhibitory assay indicated that the IC_{50} of **3** was similar to that of **12**, and 200-fold weaker than that of **11**. These data suggested that the relative configuration of two carbons (C1" and C5"), instead

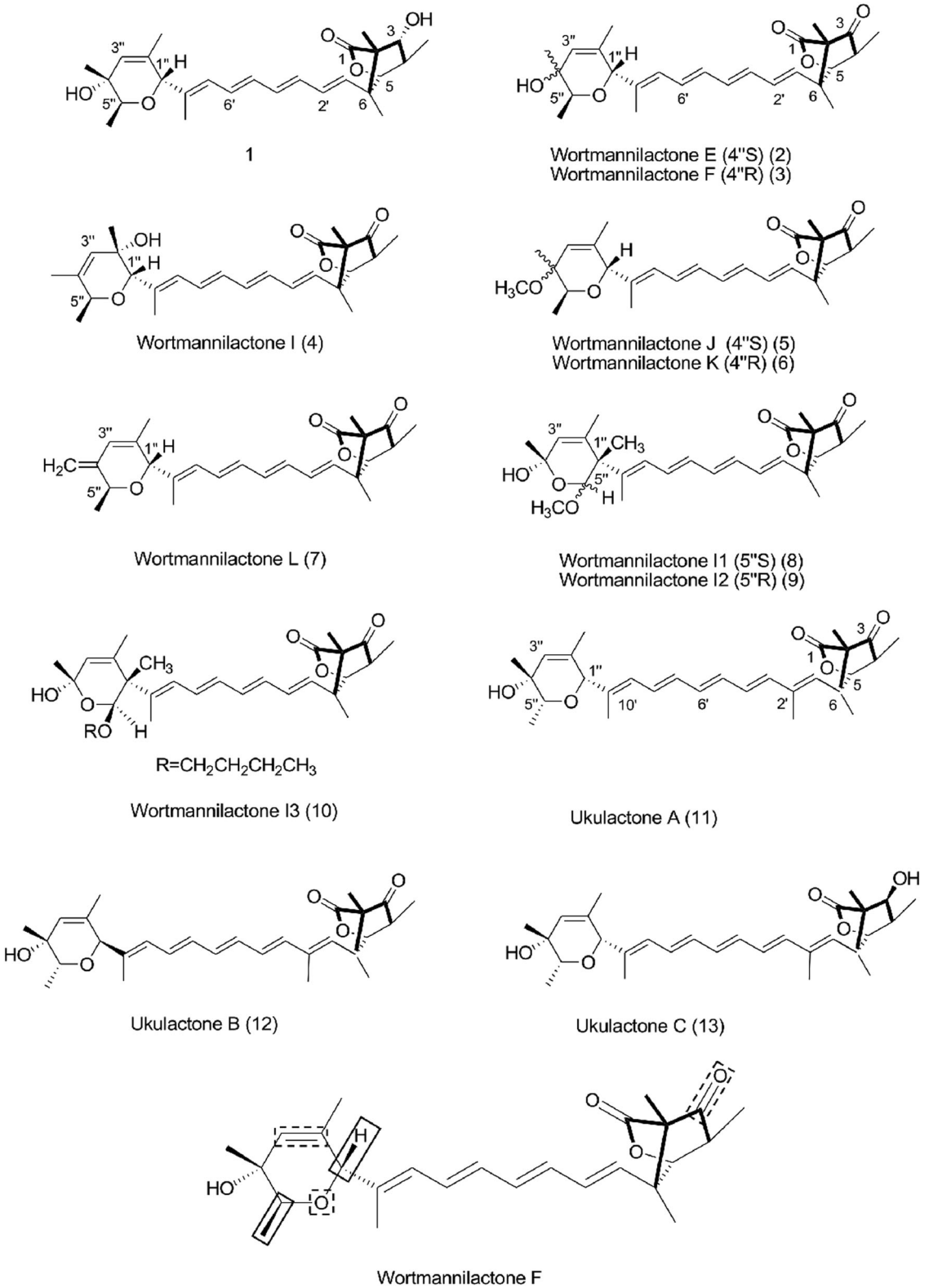

Fig. 1 The structures of wortmannilactones and ukulactones, the key groups, and relative configurations in SAR. Solid lines and dashed lines represent key relative configures and groups that affect the activity, respectively

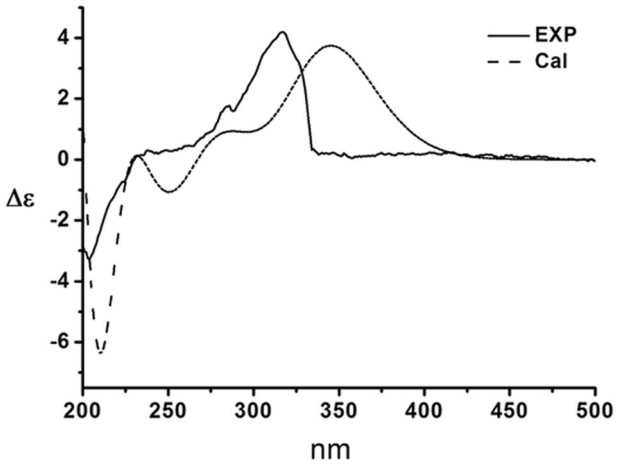

Fig. 2 Calculated and experimental ECD spectra of wortmannilactone M (dashed line, calculated at the B3LYP/6-31G (d)//B3LYP/6-31G (d, p) level in MeOH; solid line, experimental in MeOH)

carbonyl product of derivative of **11**, was 26-fold less than that of **11**[17]. As the configuration of C-3 of **1** and **13** is different, these data also suggested that the configuration of C-3 in the reduced products of wortmannilactones or ukulactones did not influence the activities significantly. The influence of the length of polyene chain on the activity of wortmannilactones was insignificant, according to the finding that **3** with a tetraene chain showed similar activities to ukulactone B with a pentaene chain.

The selective inhibitors of NFRD and complex I are mainly fungal metabolites. The common structural characteristics of these inhibitors are oxygen heterocycles conjugated with a long alkyl chain. These are proposed to compete with the substrate of complex I (rhodoquinone). The known oxygen heterocycles include δ-lactone (nafuredin) [22], 4H-pyran-4-one (verticipyrone) [23], and dihydropyran (ukulactone, wortmannilactone) [13]. However, as

Table 2 IC_{50} values of initiators against electron transport chain enzymes from submitochondrial particles of *Ascaris suum*, pig and bovine heart

Enzyme	IC_{50} (μM)													
	PP	1	2	3	4	5	6	7	8	9	10	11	12	13
NFRD from *A. suum*	0.5	13.5	0.57[a]	0.5[a]	0.85[a]	0.84[a]	1.35[a]	0.84[a]	8.8a[a]	11.0[a]	13.0[a]	0.0024[b]	0.47[b]	0.062[b]
Complex I from *A. suum*	0.4	31.0	2.0	1.0	4.0	4.0	6.0	5.0	18.0	20.0	20.0	0.055[b]	NT	NT
Complex II from *A. suum*	9.0	>100	>100	>100	>100	>100	>100	>100	>100	>100	>100	>100	NT	NT
NADH oxidase from pig or bovine heart	0.5	>100	60.0	50.0[b]	56.0[b]	100[b]	>100[b]	35.0[b]	>100[b]	>100[b]	>100[b]	9[b]	16[b]	10[b]

[a] Data from our previous work [19, 20]

[b] Data from the works of Mori and Kaifuchi [12, 17]

of the configuration of the sole carbon C1", played an important role in NFRD inhibitory activity. Compared with **3**, position changes of the oxygen atom to site 5" and the methyl substitutions of C-1"and 5"-OH in **8** and **9** led to 16-fold and 20-fold decrease in the inhibitory activity, suggesting that the oxygen position of the dihydropyran and the methyl substitution also showed positive effect on the activity. This is also supported by the fact that **5** and **6**, the methyl substituted analogs of **2** and **3** at 4"-OH, showed less activity against NFRD than those of **2** and **3**, respectively. On the other hand, the transition of the methoxyl group of C-5" to the n-butyl group (**10** vs **8**), the configuration change of C-4" (*S* in **2** vs *R* in **3**), the shift of double bonds from C-2" and C-3" to C-3" and C-4"(**3** vs **4**), or the reduction of 4"-OH to olefinic methylene (**3** vs **7**) were insignificant to the activity of the compounds against NFRD. These data suggested that these changes of the structure were insignificant.

Reducing keto-carbonyl group in the oxabicyclo [2.2.1] heptane moiety to a hydroxyl group led to a 27-fold decrease of the inhibitory activity, suggesting the importance of the keto-carbonyl group. Similar results were found in ukulactones, and the activity of **13**, which was the keto-

the structures of these inhibitors are complex with multiple chiral centers, the total or partial synthesis of NFRD and complex I inhibitors is still challenging. To our best knowledge, only nafuredin has been chemically synthesized, and the assays of its analogs demonstrated that the C-5 hydroxyl group was important for inhibitory activity. The transition of the oxygen heterocycles moiety from δ-lactone to γ-lactone did not influence the inhibition. Manipulation of metabolic processes of the producing organism by medium development, epigenetic modulation, and biotransformation by other microorganisms has been shown to be effective approaches to obtain more analogs of compounds of interest. In the present work, the assays of wortmannilactone analogs which were obtained by these means has provided important information of the SAR between wortmannilactones and electron transport enzymes, which are hopefully beneficial for the structure modification of ukulactone and wortmannilactones.

The effect of 3 on *T. spiralis*-infected mice

T. spiralis, a gut helminthic parasite exhibiting the activity of NADH-fumarate reductase [24], was selected to evaluate

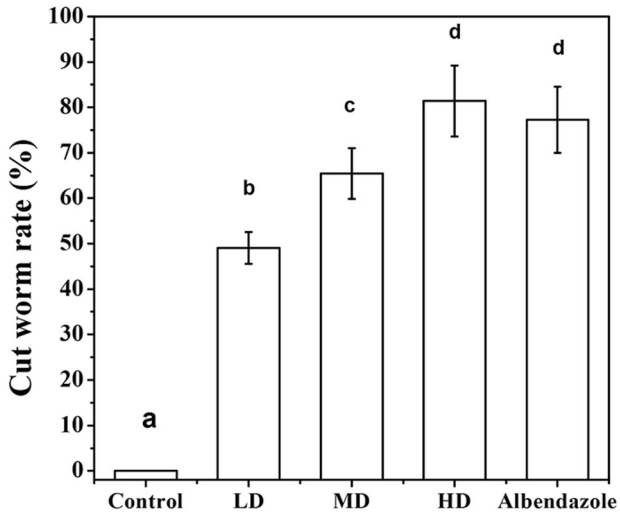

Fig. 3 The effects of wortmannilactone F on worm reduction rate in *T. spiralis*-infected mice. Control: the infected mice administrated with vehicle; LD: the infected mice administrated with 50 mg/kg/day wortmannilactone F in vehicle; MD: the infected mice administrated with 100 mg/kg/day wortmannilactone F in vehicle; HD: the infected mice administrated with 200 mg/kg/day wortmannilactone F in vehicle; Albendazole: the infected mice administrated with 25 mg/kg/day albendazole in vehicle. Values are shown as the mean ± standard deviation, $n = 8$ for each group. Values sharing different letters (**a**–**d**) in each row show statistically significant differences

the activity of **3** in vivo. Compared to the negative control group, both **3** and albendazole reduced the number of *T. spiralis* in intestinal tissue of mice ($P < 0.05$). The significant differences were found among the doses of **3** ($P < 0.05$), and the worm reduction rates were 49.1 ± 7.1%, 65.4 ± 8.5%, and 81.4 ± 9.5% for 50 mg/kg (low dose (LD)), 100 mg/kg (medium dose (MD)), and 200 mg/kg (high dose (HD)) **3** treatment, respectively. Meanwhile, the reduction rate of HD wortmannilactone treatment was not significantly different compared with the positive control, albendazole at 25 mg/kg ($P > 0.05$) (Fig. 3). These data demonstrate that **3** can treat the infection of the mice by *T. spiralis* in a dose-dependent manner.

In addition, after treatment with **3**, the length of *T. spiralis* was reduced, and the average lengths of *T. spiralis* were reduced to 2.9 ± 0.14 nm, 2.6 ± 0.17 nm, and 1.8 ± 0.2 mm in LD, MD, and HD groups, respectively, which were 14.7%, 23.5%, and 47.1% reduction than that of control and significantly reduced from the negative control group ($P < 0.05$) (Fig. S9). Hence, the effect of **3** on the size of *T. spiralis* was also dose dependent.

The effect of 3 on the histology of the worm cuticle and the microvilli in infected mice

The effects of **3** on the worm cuticle were observed by transmission electron microscopy (TEM). In the control group, the surface of the cuticle was smooth, the thickness of cuticle was even, and the distance intervals of the stripes were almost equal (Fig. 4). However, distinct changes were observed in **3**-treated groups. The shape of cuticle became rough and uneven, and the thickness of the cuticle was also decreased, suggesting that the cuticle of *T. spiralis* was damaged. The level of damage increased with higher doses of **3** (Fig. 4).

The significant changes of the microvilli of the infected mice were also observed. In the negative control group, the microvilli showed relatively coherent structures and the borders were arranged regularly. Treatment of **3** led to disintegrated structures of the microvilli, including an irregular arrangement and the loss of brush border (Fig. 5). With the increased doses of the drug, the disintegration of the microvilli became more serious. In LD drug treatment group, only part of the microvilli brush border fell off, became sparse, was different in length, and the array of microvilli was inversed. In MD group, the microvilli became shorter and smaller. In HD group, the changes were more dramatic. The microvilli intestinal epithelial cells of *T. spiralis* from different groups displayed remarkably different structures and morphology with respect to the structural integrity, the arrangement manner, the shape, and the length.

The cuticle and microvilli of adult *T. spiralis* were found to contain numerous mitochondria generating adenosine triphosphate for the worm [13, 25]. The microvilli were related to the absorption of nutrients, and the cuticle provided a defense mechanism against the attack from the immune system of the host. Previous studies indicated that inhibiting the energy metabolic pathway of *T. spiralis* by antihelminthics could induce ultrastructural changes in the cuticle [26]. In the present work, **3** was reported to reduce the number and the size of *T. spiralis* in intestinal tissue of mice in a dose-dependent manner. The ultrastructural changes of the cuticle and intestinal microvilli of *T. spiralis* caused by **3** were also observed. These data suggested that the mechanism of anthelmintic activities of **3** was to interfere with the energy metabolism of *T. spiralis* through inhibition of electron transport enzymes, leading to the destruction of the cuticle and the microvilli, and then decreasing the absorption of nutrients and the protective effect against host immune system, finally leading to the death of *T. spiralis*. Currently, the efficacy of wortmannilactones is still lower than that of albendazole. The limited water solubility and lower NFRD inhibitory activities were regarded as the main reasons. Further studies will be conducted to improve the efficacy of wortmannilactone by both introducing hydrophilic groups and structural modifications based on the SAR revealed in this work.

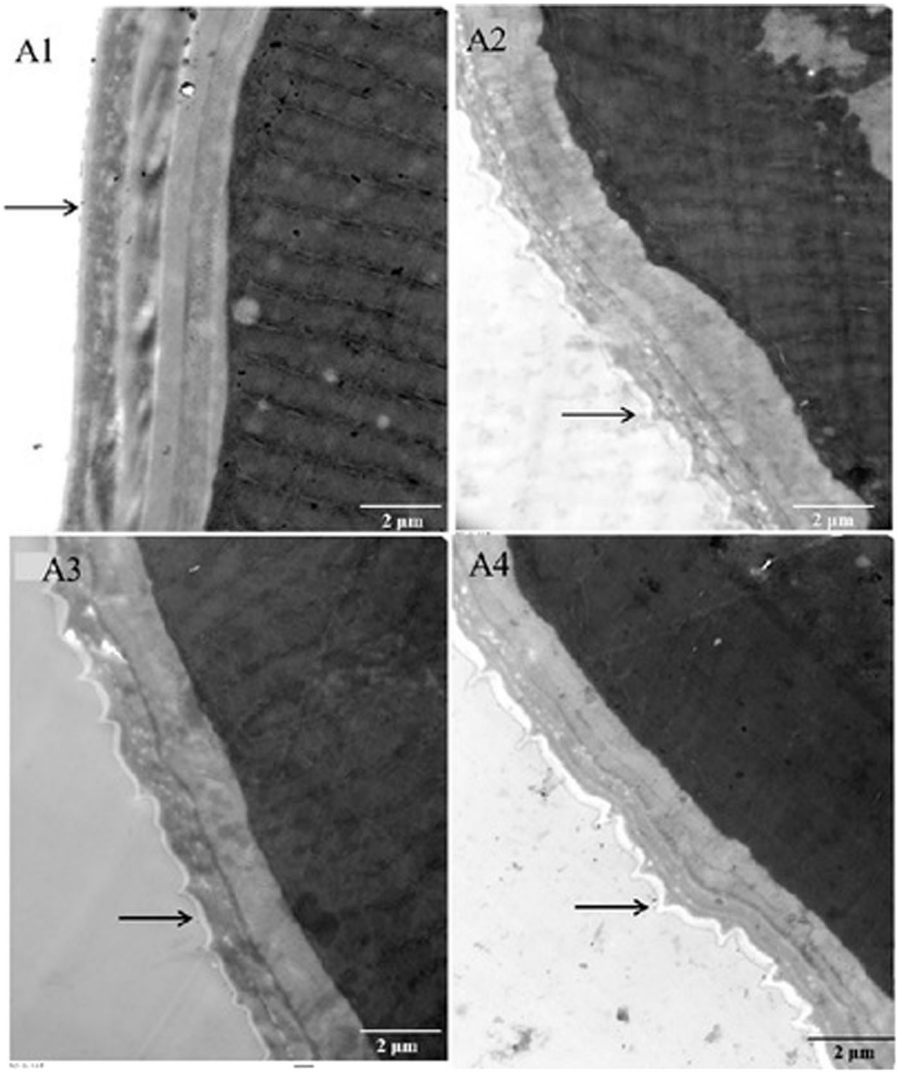

Fig. 4 The effect of wortmannilactone F on cuticles of *T. spiralis*-infected mice. A1: the infected mice administrated with vehicle; A2: the infected mice administrated with 50 mg/kg/day wortmannilactone F in vehicle; A3: the infected mice administrated with 100 mg/kg/day wortmannilactone F in vehicle; A4: the infected mice administrated with 200 mg/kg/day wortmannilactone F in vehicle. The cuticles are indicated with the arrow in each panel

Materials and methods

Materials

Thirty strains of biotransformation fungi were isolated from the sea mud collected from Heishijiao Bay (Dalian, China). High-performance liquid chromatography (HPLC) analysis was performed with the Waters HPLC system equipped with a Model 1525 pump and a Model 2998 detector. Compounds were isolated and purified by an LC3000 semi-preparative HPLC system (Beijing Chuangxin Tongheng Science and Technology Co., Ltd). DAISO ODS (SP-120-40/60-ODS-B, DAISO Co., Ltd) and YMC semi-preparative column (YMC-Pack pro C18 RS, 10 × 250 mm, 5 μm, YMC, Co. Ltd) were used for column chromatography. The NMR data were recorded with a Bruker 500 MHz spectrometer (Bruker Co). The HRESIMS data were obtained on a LTQ Orbitrap XL. The inhibition of NFRD was measured by Varioscan Flash purchased from Thermo Fisher Scientific Co. (USA). Compounds **2–10** were purified following our previous methods [19, 20], and the rhodoquinone in complex I assay was synthesized according to the published methods [27].

Male Kunming mice (16–20 g) were purchased from the SPF Laboratory Animal Center of Dalian Medical University. The mice were maintained under standard laboratory conditions. The current study protocol was approved by the international ethical guidelines and the Institutional Animal Care and Use Committee of the Dalian University of Technology.

Preparation of the biotransformation product

The 30 strains of marine-derived fungi were first revived on potato dextrose agar (PDA) medium (200 g potato/L, 20 g dextrose/L, 15 g agar/L, 30 g sea salt/L) for 3 days. Then, a single colony of each strain from PDA was inoculated in potato dextrose broth (PDB) (200 g potato/L, 20 g dextrose/

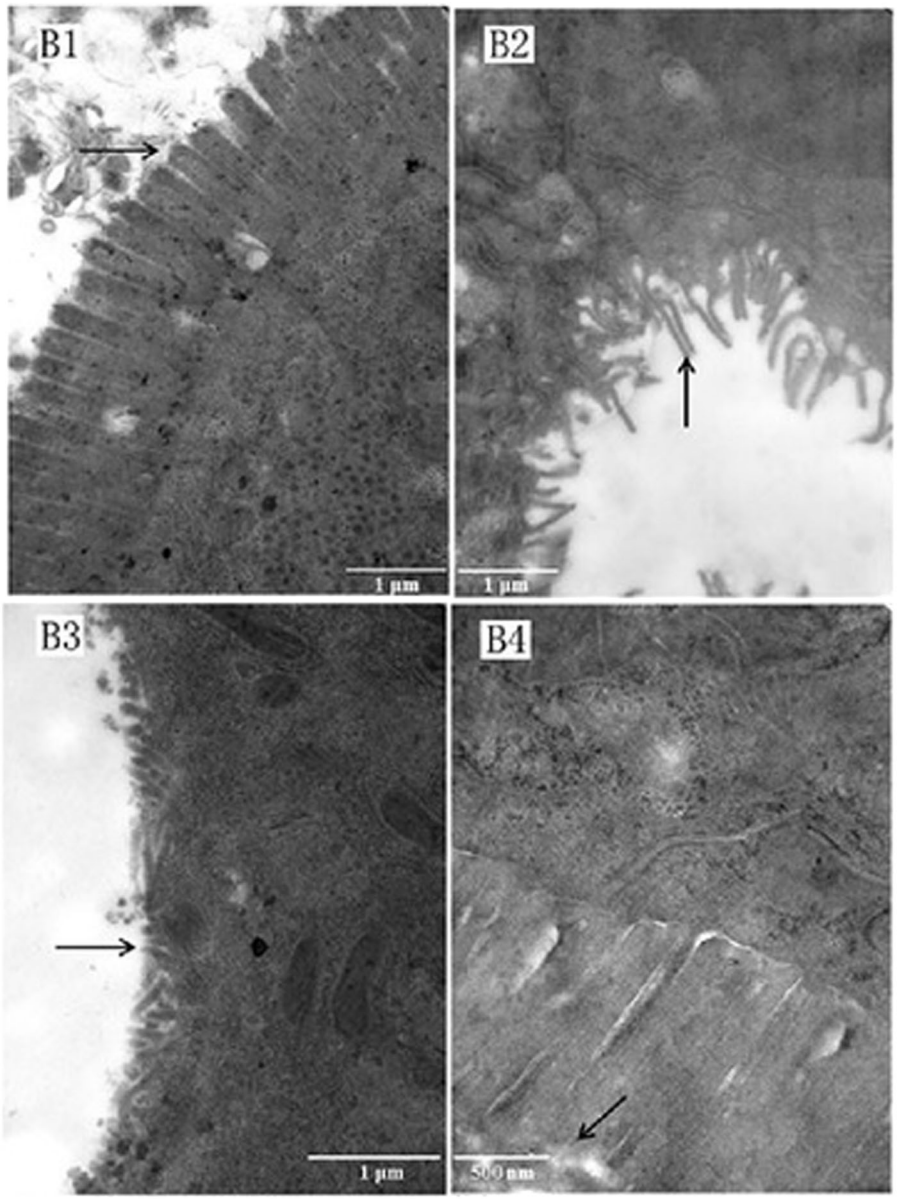

Fig. 5 The effects of wortmannilactone F on microvilli of *T. spiralis*-infected mice. B1: the infected mice administrated with vehicle; B2: the infected mice administrated with 50 mg/kg/day wortmannilactone F in vehicle; B3: the infected mice administrated with 100 mg/kg/day wortmannilactone F in vehicle; B4: the infected mice administrated with 200 mg/kg/day wortmannilactone F in vehicle. The microvilli are indicated with the arrow in each panel

L, 20 g peptone/L, and 30 g/L sea salt) and grown for 10 days. On day 3, compound **3** was added to the culture to a final concentration of 0.1 mg/mL. The fungi were grown for another 5 days, and the transformation products of 13 marine-derived fungi were detected by HPLC with a mobile phase of acetonitrile/water (volume ratio 1:1). Strain DL1103, the culture of which contained additional peaks with the characteristic ultraviolet absorption of wortmannilactones (313 nm) in HPLC-PDA analysis, was identified by ITS sequence comparison with the published data.

DL1103 was grown in 40 flasks containing PDB medium for 3 days, and then compound **3** was added to the culture to a final concentration of 0.1 mg/mL. After incubation for another 4 days, the whole culture was filtered. The filtrate was extracted three times with ethyl acetate and was evaporated under reduced pressure to harvest the dried crude extract. The dry crude extract powder (2 g) was then separated by chromatography on a DAISO ODS column (20 × 400 mm, 50 μM) with a methanol/water gradient (65% methanol to 100% methanol over 45 min) at a flow rate of 20 mL/min. A total of three fractions were generated. Fraction 2 from the ODS column was further separated by the YMC semi-preparative column (with a mobile phase of acetonitrile/water 1:1) at a flow rate of 3 mL/min to yield **1**.

Computational details

The theoretical calculations of new compounds were performed using Gaussian 09. The conformations were optimized at B3LYP/6-31G (d) level in methanol. The

theoretical calculation of ECD was performed using TDDFT at B3LYP/6-31G (d, p) level in methanol. The ECD spectra were then simulated by using a Gaussian function with band width $\delta = 0.30$ eV. The ECD spectra of new compounds were obtained by weighing the Boltzmann distribution rate of each geometric conformation.

Enzyme inhibition assay

NFRD, complex I, and complex II inhibitory activities were assayed using submitochondrial particles of *A. suum*. As other selective inhibitors against helminth electron transport chain enzymes derived from fungi are still unavailable for us, a non-selective helminth electron transport chain enzymes inhibitor, pyrvinium pamoate (PP), was used as positive control in the assay. For NFRD inhibitory activity, the muscle of *A. suum* was homogenized in phosphate-buffered saline (PBS; 50 mM, pH 7.4) and centrifuged at $1000 \times g$ for 10 min to remove the cell debris. The supernatant was further centrifuged at $10{,}000 \times g$ for 30 min and the resultant mitochondrial precipitate I was re-suspended in PBS (50 mM, pH 7.4). NADH-fumarate reductase inhibitory activity was assayed according to previous methods [13].

The mitochondrial precipitate I obtained above was re-suspended in 2 mL of PBS (50 mM, pH 7.4). The mitochondrial precipitate solution was treated by an ultrasonic homogenizer (200 W, working in cycles of 5 s on and 15 s off intervals for 90 times) and centrifuged at $15000 \times g$ for 10 min. The supernatant was further centrifuged at $40{,}000 \times g$ for 50 min and re-suspended in 1 mL PBS (50 mM, pH 7.4) to generate mitochondrial precipitate II to test the inhibitory activity against complex I and complex II.

The complex I inhibitory activity was assayed by the following system: 30 μL PBS (50 mM, pH 7.4) containing 10 mM β-D-glucose, 20 U glucose oxidase and 20 U catalase, 5 μL 0.35 mM NADH, 5 μL mitochondrial precipitate II, and 5 μL inhibitor dissolved in 2% (V/V) dimethyl sulfoxide (DMSO). The reaction was initiated by the addition of 5 μL 100 μM rhodoquinone. After an incubation at 37 °C for 15 min, the absorbance at 340 nm was determined every 20 s for 10 min at 37 °C. Complex II activity was measured in a system of 30 μL PBS (50 mM, pH 7.4) containing 20 U glucose oxidase, 20 U catalase, 10 mM β-D-glucose, and 1 mM sodium borohydride, 5 μL 100 mM decyl-rhodoquinone, 5 μL mitochondrial precipitate II, and 5 μL inhibitors dissolved in 2% (V/V) DMSO. The reaction was started by the addition of 5 μL 0.35 mM sodium fumarate. After the incubation, the absorbance at 283 nm was determined every 20 s for 10 min at 37 °C.

NADH oxidase inhibitory activity was assayed using submitochondrial particles of porcine heart. The submitochondrial particles were obtained by the same procedure to that of NFRD. The NADH oxidase inhibitory activity inhibitory activity was assayed as previously reported [13, 27].

Establishment of the *T. spiralis*-infected mice models and experimental groups

Male Kunming mice were maintained under standard laboratory conditions, fed with a normal rodent diet with free access to water for 15 days. On day 16, each mouse was infected orally with 300 encysted muscle larvae of *T. spiralis* for 5 days. A total of 32 mice were selected as infected mice. Another 8 mice were fed with a normal diet and used as the negative control. The infected mice were randomly administrated intragastrically with vehicle (5% ethyl oleate, 5% PEG 400, 10% Tween 80, 80% sterile water), 50, 100, or 200 mg/kg/day of **3**, or 25 mg/kg/day albendazole, respectively, for 3 consecutive days. On day 4, all mice were killed and dissected. The *T. spiralis* in each mouse were collected and washed with saline. The lengths of *T. spiralis* in each group were measured and the worm reduction rates were calculated according to Eq. 1. The adult worms were also stained with carmine for morphological observation.

$$\textit{Worm}\ \text{reduction rate} = \frac{\text{Number of worms in control group} - \text{Number of worms in experimental group}}{\text{Numbers of worms in control group}} \times 100\%. \quad (1)$$

Histopathological assessment

TEM (JEM-2000, EX, Japan) was performed to worms of different groups as previously reported with slight modifications. Briefly, the adult worms were fixed in 2.5% glutaraldehyde and 2% paraformaldehyde in PBS (pH 7.4). The worms were then washed with PBS for three times, 15 min each. After a fixation in 1% OsO_4 in PBS for 2 h, the samples were washed with cooled distilled water for three times and dehydrated in a concentration gradient of ethanol solutions for 15 min each. Thereafter, the worms were treated with 0.1 mL epoxy resin and blocking reagent overnight. Then, the blocking solution was changed and solidified in an incubator at a temperature gradient of 35 °C, 45 °C, and 60 °C. Subsequently, ultrathin sections were prepared and stained with uranyl acetate and lead citrate. The slides were examined and photographed by TEM.

Statistical analysis

The statistical analysis was performed using SPSS 17.0, and all results were expressed as the mean ± standard deviation. Comparisons between groups were analyzed using one-way

analysis of variance followed by Tukey's multiple comparison. The P value of less than 0.05 was considered as statistically significant.

Acknowledgements This work was supported by the National Natural Science Foundation of China (81172966). We are grateful to Dr. Jun Kun, Dalian University of Technology, for help in obtaining NMR and MS data and are grateful to Dr Yuanhua Qin, Department of Parasitology, College of Basic Medical Sciences, Dalian Medical University, for suggestions concerning the animal experiments.

Compliance with ethical standards

Conflict of interest The authors declare that they have no conflict of interest.

References

1. Hotez PJ, et al. Helminth infections: the great neglected tropical diseases. J Clin Invest. 2008;118:1311–21.
2. Otake H. Schistosomiasis: number of people treated worldwide in 2013. Wkly Epidemiol Rec. 2015;90:25–32.
3. Anthony RM, Rutitzky LI, Urban JF Jr, Stadecker MJ, Gause WC. Protective immune mechanisms in helminth infection. Nat Rev Immunol. 2007;7:975–87.
4. Robertson SJ, Martin RJ. Levamisole-activated single-channel currents from muscle of the nematode parasite Ascaris suum. Br J Pharmacol. 1993;108:170–8.
5. Dent JA, Smith MM, Vassilatis DK, Avery L. The genetics of ivermectin resistance in Caenorhabditis elegans. Proc Natl Acad Sci USA. 2000;97:2674–9.
6. Arena JP. Expression of Caenorhabditis elegans mRNA in n Xenopus oocytes: a model system to study the mechanism of action of avermectins. Parasitol Today. 1994;10:35–37.
7. Lacey E, Gill JH. Biochemistry of benzimidazole resistance. Acta Trop. 1994;56:245–62.
8. Gardner DR, Brezden BL. The sites of action of praziquantel in a smooth muscle of Lymnaea stagnalis. Can J Physiol Pharmacol. 1984;62:282–7.
9. Lewis JA, Wu CH, Berg H, Levine JH. The genetics of ivermectin resistance in Caenorhabditis elegans. Genetics. 1980;95:905–28.
10. Towers PR, Edwards B, Richmond JE, Sattelle DB. The Caenorhabditis elegans lev-8 gene encodes a novel type of nicotinic acetylcholine receptor alpha subunit. J Neurochem. 2005;93:1–9.
11. Kita K, Takamiya S. Electron-transfer complexes in Ascaris mitochondria. Adv Parasitol. 2002;51:95–131.
12. Mori M, et al. Ukulactones A and B, new NADH-fumarate reductase inhibitors produced by Penicillium sp. FKI-3389. Tetrahedron. 2011;67:6582–6.
13. Matsumoto J, et al. Anaerobic NADH-fumarate reductase system is predominant in the respiratory chain of Echinococcus multilocularis, providing a novel target for the chemotherapy of alveolar echinococcosis. Antimicrob Agents Chemother. 2008;52:164–70.
14. Sakai C, Tomitsuka E, Esumi H, Harada S, Kita K. Mitochondrial fumarate reductase as a target of chemotherapy: From parasites to cancer cells. Biochim Biohpys Acta. 2012; 1820:643–51.
15. Omura S, et al. An anthelmintic compound, nafuredin, shows selective inhibition of complex I in helminth mitochondria. Proc Natl Acad Sci USA. 2001;98:60–62.
16. Lang G, Wiese J, Schmaljohann R, Imhoff JF. New pentaenes from the sponge-derived marine fungus Penicillium rugulosum: structure determination and biosynthetic studies. Tetrahedron. 2007;63:11844–9.
17. Kaifuchi S, Mori M, Nonaka K, Masuma R, Ōmura S, Shiomi K. Ukulactone C, a new NADH-fumarate reductase inhibitor produced by Talaromyces sp. FKI-6713. J Gen Appl Microbiol. 2015;61:57–62.
18. Dong YS. et al. Cathepsin B inhibitory tetraene lactones from the fungus *Talaromyces wortmannii*. Helv Chim Acta. 2009;29:567–74.
19. Liu WC, et al. Wortmannilactones I–L, new NADH-fumarate reductase inhibitors, induced by adding suberoylanilide hydroxamic acid to the culture medium of Talaromyces wortmannii. Bioorg Med Chem Lett. 2016;26:5328–33.
20. Liu WC, et al. Production of polyketides with anthelmintic activity by the fungus Talaromyces wortmannii using one strain-many compounds (OSMAC) method. Phytochem Lett. 2016;18:157–61.
21. Tomitsuka E, Kita K, Esumi H. An anticancer agent, pyrvinium pamoate inhibits the NADH–fumarate reductase system-a unique mitochondrial energy metabolism in tumour microenvironments. J Biochem. 2012;152:171–83.
22. Ui H, et al. Nafuredin, a novel inhibitor of NADH-fumarate reductase, produced by Aspergillus niger FT-0554. J Antibiot. 2001;54:234–8.
23. Shiomi K, et al. Verticipyrone, a new NADH-fumarate reductase inhibitor, produced by Verticillium sp. FKI-1083. J Antibiot. 2006;59:785–90.
24. Rodriguez-Caabeiro F, Criado-Fornelio A, Jimenez-Gonzalez A. A comparative study of the succinate dehydrogenase-fumarate reductase complex in the genus Trichinella. Parasitology. 1985;91 (Pt):577.
25. Kita K, Hirawake H, Miyadera H, Amino H, Takeo S. Role of complex II in anaerobic respiration of the parasite mitochondria from Ascaris suum and Plasmodium falciparum. Biochim Biohpys Acta. 2002;1553:123–39.
26. Matadamas-Martínez F, et al. Analysis of the effect of a 2-(trifluoromethyl)-1 H -benzimidazole derivative on Trichinella spiralis muscle larvae. Vet Parasitol. 2013;194:193–7.
27. Moore HW, Folkers K. Coenzyme Q. LXII. Structure and synthesis of rhodoquinone, a natural aminoquinone of the coenzyme Q group 1. J Am Chem Soc. 1965;87:1409–10.